Ethyl Viologen as a Superoxide Quencher to Enhance the Oxygen Reduction Reaction in Li-O_2 Battery

Sisi Wu[#, a, b], Jing Yang[#, c], Ning Qin[a], Yingzhi Li[a], Haiou Wang[a], Yongwei Zhang[*, c], Qing Wang[*, b], Zhouguang Lu[*, a]

[a]*Department of Materials Science and Engineering, Shenzhen Key Laboratory of Interfacial Science and Engineering of Materials, Southern University of Science and Technology, Shenzhen, 518055 Guangdong, P. R. China*

[b]*Department of Materials Science and Engineering, Faculty of Engineering, National University of Singapore, Singapore 117576*

[c]*Institute of High-Performance Computing, A*STAR, Singapore 138632, Singapore*

** Corresponding author.*

E-mail address: luzg@sustech.edu.cn; qing.wang@nus.edu.sg; zhangyw@ihpc.a-star.edu.sg

ABSTRACT: LiO_2 is a critical intermediate of oxygen reduction reaction (ORR) in nonaqueous Li-O_2 battery that largely determines the discharge capacity and cycling stability. Currently, bifunctional redox mediators that can promote solution reaction route by enhancing the solvation

of LiO_2 have attracted tremendous interests in a bid to increase the attainable capacity. However, the prolonged lifetime of LiO_2 may cause instability of the battery system. Conversely, redox mediators that quench LiO_2 and facilitate surface reaction route receives little attention. Here, we provide in-depth exploration of the catalytic pathway and effect of a bifunctional superoxide quencher that facilitates the surface growth of Li_2O_2. Surprisingly, the predominant surface reaction route by EV helps deliver a capacity as much as that facilitated by solution reaction route. The findings of this work provide a new direction of screening and evaluating functioning redox mediators for Li-O_2 batteries.

INTRODUCTION

Spanning from the large-scale stationary energy storage to the electrification of transportation, the ever-growing demand for sustainable energy storage and conversion devices with high energy density skyrockets in the recent decades.[1-3] In pursuit of qualified energy sources, particular interests have been spurred to develop various electrochemical energy storage (EES) systems, among which Li-O_2 batteries are promising because of the ultrahigh energy density.[4] However, the advancement of Li-O_2 batteries has long been plagued by the low energy efficiency, compromised attainable capacity and inferior cycling stability.[5-9] One of the culprits lies on the cathode side, especially the sluggish oxygen reduction reaction (ORR) and oxygen evolution reaction (OER).

Realizing their ultrahigh theoretical energy density is the ultimate target in studying Li-O_2 batteries. Hitherto, all kinds of functioning heterogeneous electrocatalysts have been explored to improve the reaction kinetics. However, the insulating Li_2O_2 tends to block the gas access and deactivate the coated catalysts at an early stage of a discharge process. Such passivation severely compromises the attainable capacity of a Li-O_2 battery. Recently, boasting their soluble nature and

flexible chemical composition, soluble catalysts stand out as promising catalysts for Li-O_2 batteries. Soluble catalysts, also called redox mediators (RMs), allow the formation and decomposition of Li_2O_2 dissociated from the cathode surface by acting as an electron shuttle.[10-19] Their soluble nature protects them from deactivation throughout the battery operation, thus alleviating the passivation-led capacity compromise.

Another essential determinant of the capacity is the LiO_2 intermediates during the discharge process. Prevailingly, solution reaction route is preferred to surface reaction route because the LiO_2 intermediates can stay solvated longer and survive before migrating to existing Li_2O_2 particles for further growth. Since solution reaction route mitigates the cathode passivation to some degree and allows a much larger capacity compared to surface reaction route, bifunctional RMs which can promote solution reaction route as a superoxide shuttle are attracting tremendous interests.[17-24] However, the enhanced solvation of reactive LiO_2 intermediates by these RMs could bring about parasitic reactions which are another central issue of Li-O_2 batteries besides attainable capacity. Among the previously reported bifunctional RMs, only few were demonstrated to mitigate the parasitic reactions with increased yield of Li_2O_2. Whether or not the promoted solution reaction route facilitated by RMs weakens the stability of Li-O_2 batteries remains an open question. To address such an issue, we determine to explore superoxide-quencher type RMs which have the potential to eliminate parasitic reactions from LiO_2.

In 2015, Owen group stated that ethyl viologen (EV) can both catalyze ORR and shorten the life span of superoxide anions as EV^+ reduces oxygen species (O_2 and LiO_2).[14] Such a redox mediator received little attention, presumably because the proposed catalytic pathway of EV favours the surface reaction route which is believed unprofitable for capacity, and its influence on the reaction route remains unclear. Different from the previously reported RMs that are pertinent to LiO_2, it

also arouses our curiosity about its potentially unique catalytic pathway and effect. Inspired by this work, we determine to unravel the reaction between EV^+ and LiO_2 and scrutinize the impact of EV on the discharge performance of Li-O_2 batteries.

In this work, we provide both computational and experimental evidence of EV^+ in reducing LiO_2 to Li_2O_2. With the assistance of rotating ring-disk electrode (RRDE), the reaction between EV^+ and LiO_2 was well rationalized, which is in accordance with the density functional theory (DFT) calculations that electrons were found to transfer from EV^+ to LiO_2 during the reaction. The addition of EV also promoted the surface reaction route even through different discharge modes, in which the morphological difference of the discharge products was well correlated to the catalytic pathway. Surprisingly, along with the predomination of surface reaction route, a large discharge capacity, which is comparable to the condition with solution reaction route, can be achieved as well.

RESULTS AND DISCUSSION

First, the catalytic effect of EV was examined by cyclic voltammetry (CV). As shown in Fig. S1, the redox couple of EV^{2+}/EV^+ presents a reversible redox potential at 2.52 V vs. Li/Li^+, which suits to catalyze ORR. When the electrolyte was saturated with O_2, the enhancement of the reduction and the suppression of the oxidation suggest the typical electrochemical-chemical (EC) ORR process. Taking advantage of the radical property of EV^+, electron paramagnetic resonance (EPR) was also used to probe the electron flow from EV^+ to O_2. Lacking unpaired electrons, the pristine EV^{2+} does not present any radical property, while the extra electron renders a distinct radical response with EV^+ (Fig. S2a). The subsequently supplied O_2 quenched the radical response,

suggesting that O_2 intercepted the unpaired electron from EV^+. The concurrently appeared sharp peak along with the vanishing radical signal of EV^+ can be assigned to the oxygen-rich states of Li_2O_2.[25, 26] Apart from EV itself, we also monitored and compared the evolution of LiO_2 produced during the ORR processes (Fig. S2b). With the assistance of the radical trapping reagent, DMPO, LiO_2 was detected during the both ORR processes. It is worth noting that the addition of EV produced much concentrated LiO_2, indicating a much faster ORR reaction rate due to the catalysis. Therefore, both the CV results and the radical analysis compellingly prove that EV can function as a RM to promote ORR.

According to Owen's findings[14], EV^+ is capable of reducing KO_2, while whether a similar superoxide quenching process can occur to LiO_2 remains unclear. Therefore, DFT calculations were carried out to study the Li_2O_2 growth reaction mechanism with special attention on the electron transfer between EV^+ and the intermediates. Details for the DFT procedures, EV and intermediate model selections and ORR process modelling can be found in the supporting information. By carefully examining the frontier orbitals before and after the interaction (Fig. S5), we conclude that the EV^+ plays the role of electron donor and O_2-$(Li_2O_2)_5$ is the electron acceptor, which are in accordance with the typical EC process observed from CV and EPR spectra.

The detailed frontier orbitals before and after the interactions between EV^+ and LiO_2-$(Li_2O_2)_5$ are summarized in Fig. 1. The structure of clean LiO_2-$(Li_2O_2)_5$ is shown is Fig. 1a. The highest occupied molecular orbital (HOMO) of EV^+-LiO_2-$(Li_2O_2)_5$ (Fig. 1c) shares the similar feature as the lowest unoccupied molecular orbital (LUMO) of LiO_2-$(Li_2O_2)_5$ (Fig. 1b). The only difference between them is that such a molecular orbital is empty before interaction but occupied after the interaction. This suggests that during the interaction, electrons of EV^+ have been injected into

LiO_2-$(Li_2O_2)_5$. On the other hand, the LUMO of EV^+-LiO_2-$(Li_2O_2)_5$ is mainly composed of HOMO of EV^+, which indicates that EV^+ works as an electron donor during the interaction between EV^+ and LiO_2-$(Li_2O_2)_5$. In short, by comparing the difference in the frontier orbitals, we conclude that the electrons flow from EV^+ to LiO_2-$(Li_2O_2)_5$ during their interaction. The electron transfer is further confirmed by the comparison of the HOMO of EV^+-LiO_2-$(Li_2O_2)_5$ (Fig. 1c) and HOMO of O_2-$(Li_2O_2)_5$ anion (Fig. 1f). Their HOMOs share identical features, which indicates that the consequence of interacting with EV^+ is the same as the whole system with extra electrons, which again supports that the EV^+ plays the role of electron donor and it donates electrons to LiO_2-$(Li_2O_2)_5$. The amount of charge transfer is then confirmed by the Mulliken charge calculation, as shown in Fig. 1g. During the interaction, 0.22 e^- is transferred from EV^+ to LiO_2-$(Li_2O_2)_5$. Such a charge transfer is in good accordance with our experimental observation that EV^+ plays as a reductant during the ORR reaction. It is interesting to note that the net charge of newly attached O_2 is -0.91 e^-, which is closer to the net charge of peroxide. Compared with the -0.61 e^- net charge of the adsorbed O_2 in EV^+-O_2-$(Li_2O_2)_5$ system (Fig. S5f), a higher net charge of -0.91 e^- suggests the electron injection into this newly adsorbed O_2 group. This adsorbed O_2 group firstly gets -0.61 e^- from EV^+ (Fig. S5f) and further gets more electrons from another EV^+ to make the whole net charge of the O_2 group up to 0.91 e^- (Fig. 1f). Such a step-by-step reduction of the O_2 group agrees well with our experimental observation that the O_2 group is reduced first to superoxide and then peroxide. A periodic slab model has also been applied to further confirm the charge transfer between EV^+ and LiO_2-$(Li_2O_2)_5$ and the results are summarized in Figure S6(b). The electron density difference map clearly shows that during the interaction, the electrons flow from EV^+ to the surface adsorbed O_2.

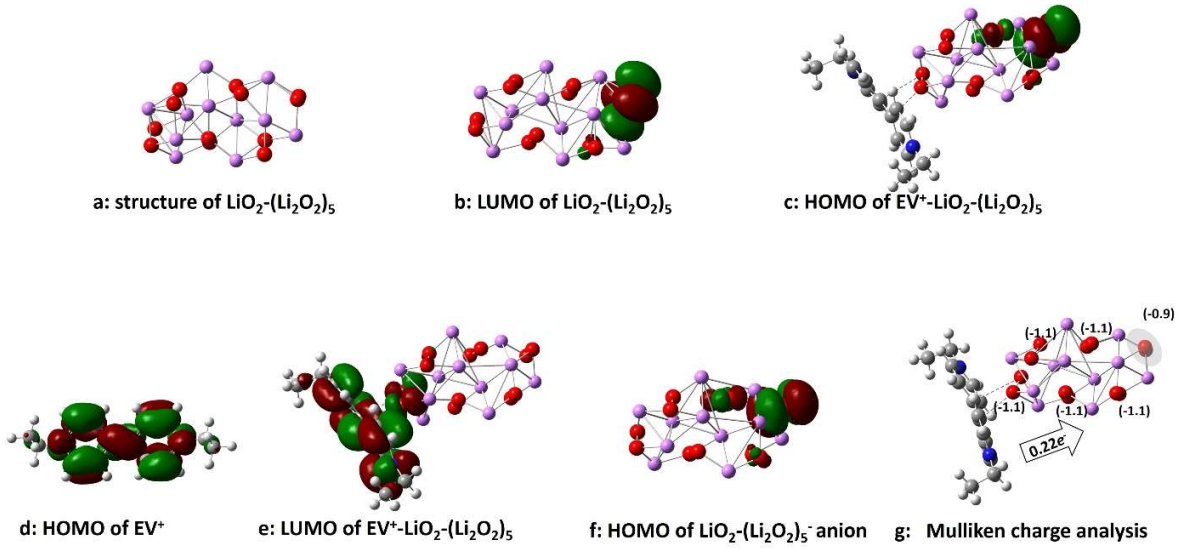

Figure 1. Detailed comparison of frontier orbital before and after the interaction between EV^+ and LiO_2-$(Li_2O_2)_5$ cluster. (a) optimized structure of LiO_2-$(Li_2O_2)_5$. (b) LUMO of LiO_2-$(Li_2O_2)_5$. (c) HOMO of EV^+-LiO_2-$(Li_2O_2)_5$. (d) HOMO of EV^+. (e) LUMO of EV^+-LiO_2-$(Li_2O_2)_5$. (f) HOMO of LiO_2-$(Li_2O_2)_5$ anion. (g) The charge transfer predicted with the Mulliken charge calculation. The net charge (in e^-) of the O-O groups is labeled in the parentheses. The charge transfer direction and amount are shown in the blue arrow. Red, purple, blue, grey and white spheres represent O, Li, N, C and H atoms, respectively.

The potential energy surface of Li_2O_2 formation with the assistance of EV^+ is shown in Fig. 2. O_2 is firstly adsorbed to the cluster via an exothermic process with an energy change of 0.56 eV. Afterwards, the adsorbed O_2 is reduced by EV^+ to form LiO_2 intermediate exothermically by 1.13 eV. When further reacting with another EV^+, LiO_2 is reduced to Li_2O_2, which gives out energy of 1.21 eV. Each step is downward in energy, suggesting a thermodynamically favored reduction procedure during which EV^+ participates in both the reductions. In other words, EV^+ can serve as both electron shuttle and superoxide quencher that facilitate both reductive steps in an individual ORR. It is worth noting that the reaction between EV^+ and LiO_2 should, in theory, accelerates the formation and precipitation of Li_2O_2, which may promote the surface reaction route and exacerbate the cathode passivation.

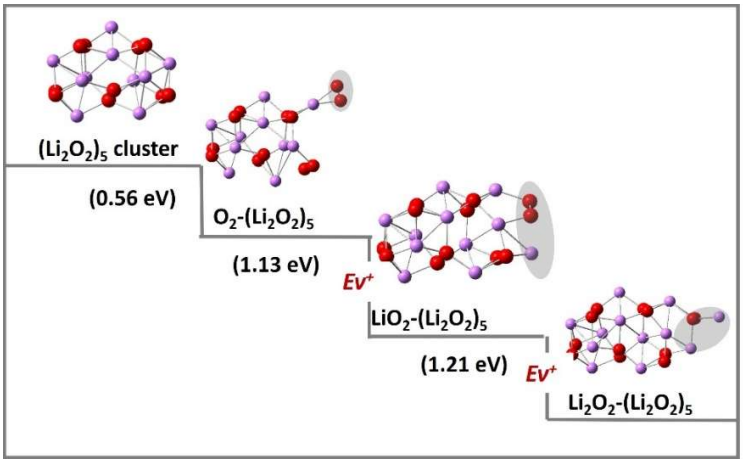

Figure 2. The potential energy surface of Li_2O_2 formation predicted with $(Li_2O_2)_5$ cluster model. The red and purple spheres represent oxygen and lithium atoms, respectively. The atoms under shadow denoted the Li_2O_2 growth pathway. The reaction energy (in eV) for each step is shown in parentheses.

Based on the calculated electron flow and free energy diagram, it is rational to describe the catalytic reaction pathway as below, which is in accordance with Owen's study derived from KO_2[14]:

$$EV^{2+} + e^- \longrightarrow EV^+ \quad (1)$$

$$EV^+ + Li^+ + O_2 \longrightarrow EV^{2+} + LiO_2 \quad (2)$$

$$EV^+ + Li^+ + LiO_2 \longrightarrow EV^{2+} + Li_2O_2 \quad (3)$$

According to this catalytic pathway, EV^+ molecules are responsible for reducing both O_2 and LiO_2, both expediting the ORR process and exacerbating the passivation. Apart from the evidence from the DFT calculations, experimental evidence was also collected to elucidate the interaction between EV^+ and LiO_2. As shown in the CV curve (Fig. S1), the presence of O_2 rendered a noticeable ~0.125 V negative shift in E_p of the reduction of EV, which presumably results from the passivation of the electrode surface by Li_2O_2 precipitation, while negligible shift was observed

for the reported superoxide shuttle, duroquinone (DQ)[19, 22] and 2,5-di-tert-butyl-1,4-benzoquinone (DBBQ)[17] regardless of the presence of O_2. In line with the role of superoxide shuttle, these quinones consequently prolong the lifetime of solvated O_2^-, mitigating the passivation during the cathodic and thus having a negligible polarization. It is thus rational to attribute the severe passivation observed with EV to the accelerated Li_2O_2 deposition.

Rotating disk-ring electrode (RRDE) measurements are an important and efficient approach to reveal the underlying chemistry between EV^+ and LiO_2. Fig. S8 illustrates the working mechanism of this measurement. The collection efficiency $N_k = i_r/i_d$ evaluates the ratio of the reduced species and pristine oxidized species. Comparing the N_k obtained in the absence and presence of O_2 can provide meaningful information of the underlying chemistry of the EV-catalyzed ORR. Fig. 3a shows the linear sweep voltammetry (LSV) curves of EV in Ar and O_2-saturated electrolytes. In the absence of O_2, i_d reaches the diffusion-limited condition, followed by the second reduction (EV/EV^+) at ~1.9 V. In the presence of O_2, one apparent reduction peak of EV^+/EV^{2+} was observed while the diffusion-limited state was yet reached. In addition, the ring current i_r was suppressed to a great extent, along with the reduction of N_k from 0.277 to 0.088. Such a reduction of N_k can be rationalized with a lowered concentration of reduced species (both EV^+ and LiO_2) on the ring electrode, indicating a process consuming these two species after their formation on the disk electrode. Fig. 3b presents the LSV curves of EV at the disk electrode in the presence of O_2. With the descending rotation rate, despite the initial large reduction current observed at 2500 rpm, the currents of the following curves are surprisingly suppressed. Even though the diffusion limited condition was not reached, we also tentatively presented the Koutecky-Levich plots with the maximum current density obtained at each rotation rate (Fig. 3d), and the number of electrons transferred (n) was calculated to be approx. 0.2 based on the Koutecky-Levich equation with the

parameters determined in previous research.[12, 27] Even though the plot broadly suggests a linear relation, the electron transfer was way less than the theoretical value, 1. Given the electrolyte convection caused by electrode rotation, obviously there was a process other than mass transport limiting the current. Here, a surface process such as electrode passivation (pathway 3) would plausibly be the root cause of such current suppression. To verify the above analysis, the same LSV measurements were conducted in the absence of EV (Fig. 3c). Comparatively, the disk currents remain obvious at low rotation rates, presumably due to the comparatively less passivated scenario without EV. In addition, n was calculated to be approx. 0.86 in the absence of EV (Fig. 3d), which is much higher than the value obtained in the presence of EV and much nearer to 1. Such a difference of n is also explainable by the exacerbated passivation triggered by EV^+, which can be attributed to the accelerated Li_2O_2 deposition by the reaction between EV^+ and formed LiO_2. Hence, the above discussion rationalizes the reaction between EV^+ and LiO_2 in forming insoluble and insulating Li_2O_2, which reduces the concentration of both species and passivates the disk electrode surface in the subsequent measurement as well.

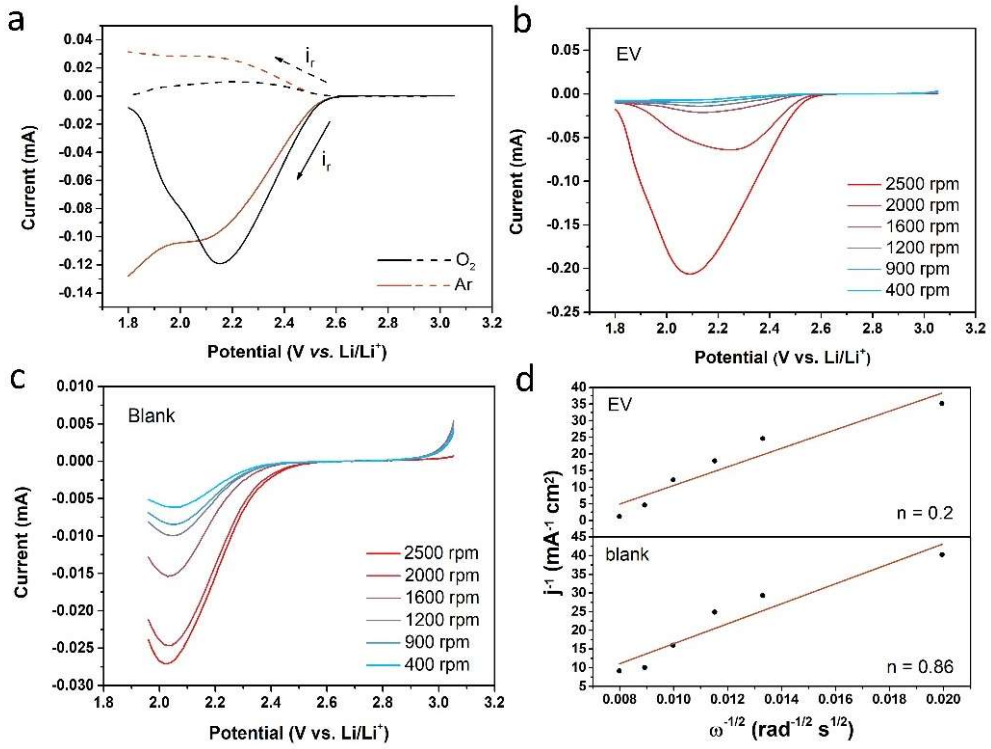

Figure 3. (a) Linear sweep voltammetry (LSV) curves of EV in Ar- and O_2-saturated electrolyte. The rotation rate was 400 rpm. LSV curves at disk of (b) EV and (c) blank in O_2-saturated electrolyte at descending rotation rate. Linear potential from 3.2 V to 1.8 V (vs. Li/Li^+) was applied to the disk electrode and 3.5 V (vs. Li/Li^+) was fixed at the ring electrode. The scan rate was 10 mV s^{-1}. The concentration of the redox mediator was 5 mV and the supporting electrolyte was 0.1 M LiTFSI in TEGDME. (d) Koutecky-Levich plots (dot) and fitted line (red) of EV and blank based on the current densities at each rotation chosen corresponding to the E_p at 2500 rpm.

Time-dependent retention of LiO_2 was also monitored by electron paramagnetic resonance (EPR) spectroscopy for a direct observation of the interplay between EV species and LiO_2. Fig. 4 shows the retention of LiO_2 produced with DQ^-, EV^+ and in the absence of redox mediator (denoted as blank). It is not surprising to see that the retention of O_2^- produced with DQ^- maintains stably around 100%, while it drops quickly to zero at the halfway in the blank case, which indicates the short lifetime of LiO_2 in low DN solvents.[8, 28] However, the trend for the EV case remains not entirely clear considering the fluctuation and large error bars (Fig. 4b). Broadly the retention of

LiO_2 signal is attenuated compared with that of DQ while the decay is considerably slowed compared with the blank case. Considering the broadly scattered and overall declined signal, it is rational to assume that there are competitive reactions for the EV system, some of which produce LiO_2 and others consume it. Based on the proposed catalytic pathway and the conclusion drawn from the RRDE analysis, we speculate that it was the competition between pathway (2) and pathway (3) that dominated during the EPR measurements. Since excess O_2 had been previously bubbled to the electrolyte, there was abundant remaining O_2 after the electrochemical reduction, which continuously helped produce LiO_2 during the relaxation time. Meanwhile, the reduced EV^+ can also react with the produced LiO_2 to produce Li_2O_2.

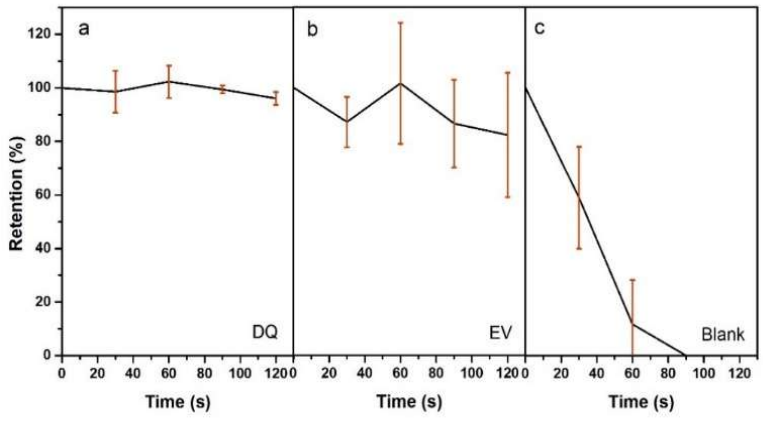

Figure 4. Time-dependent retention and its error bar of superoxide produced with (a) DQ^-, (b) EV^+ and (c) without redox mediators (denoted as blank). The value at each time in the figure is the average of calculated intensities of three individual tests. For each test, the calculated intensity was the average of the intensity of each peak to minimize the measuring errors. DMPO was added after the relaxation and before the measurements.

The impact of EV on the discharge performance of aprotic Li-O_2 batteries was examined with a quasi-Li-O_2 battery with lithium iron phosphate (LFP) as both counter and reference electrodes. As shown in Fig. 5a and b, the addition of EV exhibits positive influence in terms of both

polarization and capacity of the discharge process at different current densities. The reduced polarization results from the electron shuttling function of EV. The discharge products were further characterized by X-ray diffraction (XRD) and Raman spectroscopy (Fig. 8c and d). Both results of carbon felts discharged with and without EV suggest Li_2O_2 as the main product.

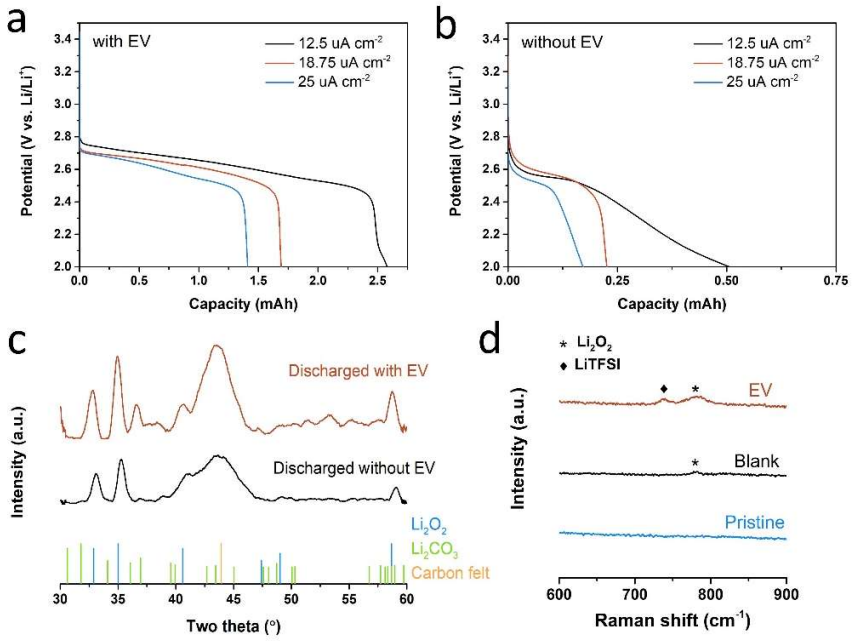

Figure 5. Load curve of O_2 reduction (a) with and (b) without EV at different current densities. The reference electrolyte was 1 M LiTFSI-TEGDME. (c) XRD patterns and (d) Raman spectra of the discharged carbon felt with (red) and without (black) EV.

In line with the interactions between EV^+ and LiO_2 intermediates, the morphology of the discharge product was another important aspect to investigate. Compared with the carbon felt discharged without EV (Fig. 6b), the addition of EV did not change the morphology of Li_2O_2 as no obvious particles were observed (Fig. 6c), indicating the predominance of surface reaction route during both the discharge processes. However, the addition of EV thickened the observable thin film with the appearance of small particles, which is supported by the enlarged capacity. To magnify the

effect of accelerated Li_2O_2 formation, galvanostatic intermittent titration technique (GITT) measurements were conducted to further disclose the function of superoxide quencher of EV. While the continuous discharge led to a thickened film (Fig. 6c), large number of small particles emerged when it comes to GITT measurements (Fig. 6d). Both morphologies conform with the features of surface reaction route,[17, 29] suggesting the constant reaction route regardless of the discharge mode. More importantly, the accumulative capacity obtained from GITT (~3.2 mAh) does not distinctly exceed the value from continuous discharge (~2.5 mAh), which seemingly contradicts the noticeable morphology change observed by SEM. Hence, a different underlying chemistry instead of the concentration polarization may be the cause of the different morphologies observed with the different discharge modes, which corresponds to the unlimited reaction between EV^+ and LiO_2 during the relaxation.

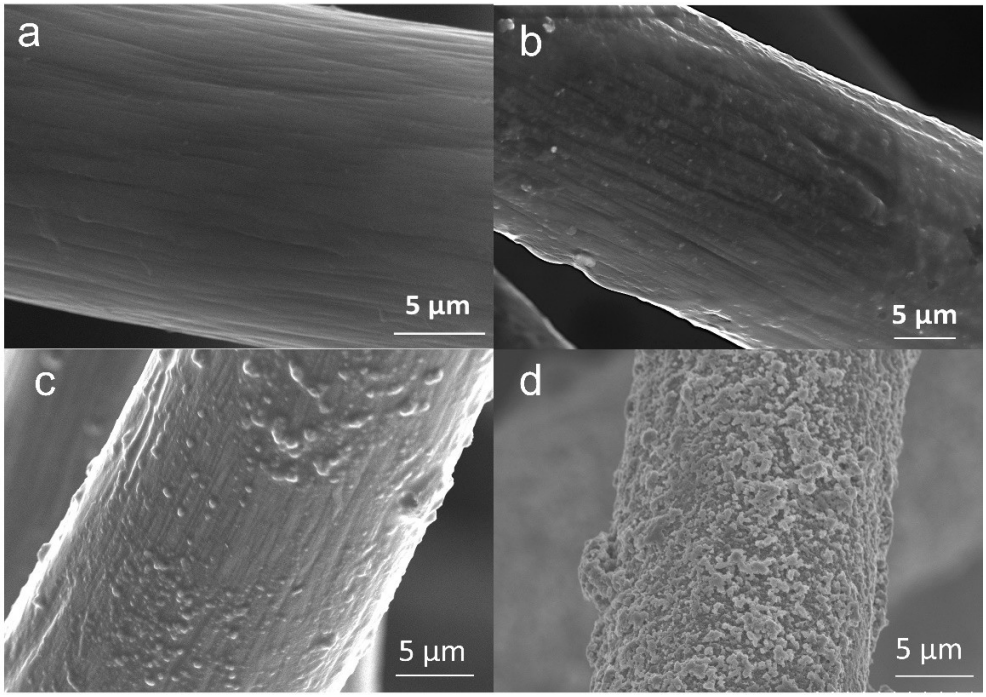

Figure 6. Scanning electron microscopy (SEM) images of (a) pristine carbon felt, carbon felts discharged (b) without and (c) with EV and (d) carbon felt after galvanostatic intermittent titration technique (GITT) test with EV.

Fig. 7 illustrates the reaction pathway during the GITT measurements. During the discharge period, EV^+ participated in the reductions of both O_2 and LiO_2 (pathways 2 and 3), accelerating the deposition of Li_2O_2 as a thick film. At the end of discharge period, large amount of LiO_2 remained accumulated and unreacted since the production of EV^+ was paused. Due to their high concentration, the superfluous LiO_2 migrated to and accumulated in the vicinity of the cathode surface, where they disproportionated to the insoluble Li_2O_2.

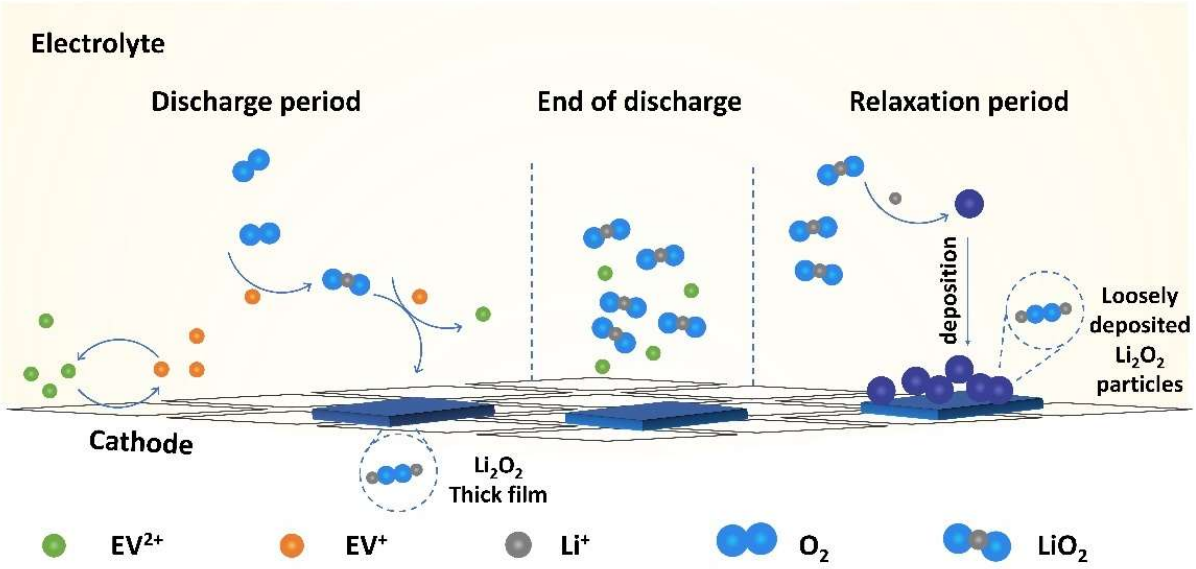

Figure 7. Schematic illustration of the reaction pathway of GITT measurement.

During the relaxation period, the disproportionation continuously occurs because of the instability of LiO_2 in TEGDME, rendering the deposition of small Li_2O_2 particles onto the cathode surface, which is observed as loosely packed flakes. The key factor is the much higher LiO_2 concentration, otherwise merely film-like Li_2O_2 deposition will be observed like the situation with continuous discharge without EV. In stark contrast, the unlimited EV^+ produced in the continuous discharge

restricts LiO_2 at the cathode surface by reducing them to Li_2O_2 immediately after their formation, leading to a thick Li_2O_2 film. Hence, it is plausible that the morphology difference caused by the different discharge modes is attributed to the reaction between EV^+ and LiO_2, echoing the above analysis of EV as superoxide quencher.

In a bid to elucidate the unique catalytic pathway of such superoxide quencher, Fig. S10 illustrates the three different ORR processes in low DN solvents. It is surprising to note that even though the surface reaction route dominates and is promoted with a superoxide quencher, the addition of EV did not compromise the delivered capacity compared with the value obtained with a superoxide shuttle (DQ, Fig. 8). This phenomenon is seemingly contradictory to the expected exacerbated cathode passivation brought by the promoted surface reaction route. Owen *et al.* attributed it to the formation of Li_2O_2 away from the cathode surface.[14] We believe that it is also rational to attribute it to the soluble nature of EV^+ that helps access the cathode surface and avoid its deactivation. The study of the immunity of deactivation can be important and it requires further efforts to investigate the underlying mechanism. The shortened lifetime of LiO_2 can be beneficial to a highly stable rechargeable Li-O_2 battery with negligible side reactions, while the attainable capacity is not compromised.

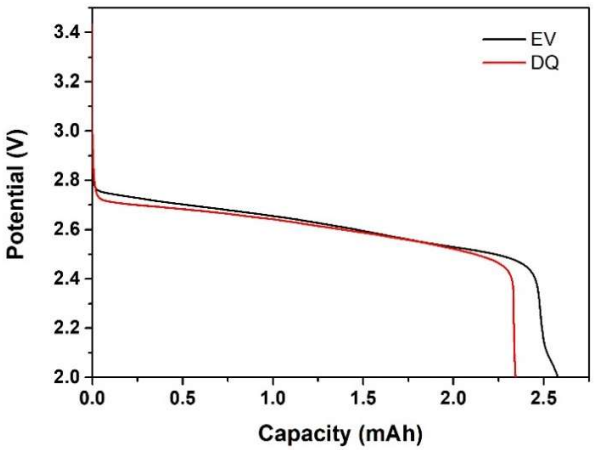

Figure 8. Load curves of O_2 reduction with DQ (red) and EV (black) at 12.5 μA cm^{-2}.

CONCLUSION

In this study, we probe the catalytic pathway and effect of EV, a superoxide quencher. We provide both computational and experimental evidence to prove the electron flow during the catalytic reaction. Suggested by the DFT calculations, EV^+ successively reduces O_2 and LiO_2, expediting the precipitation of Li_2O_2 via the surface reaction route. The reaction with EV^+ shortens the lifetime of LiO_2, which enables EV^+ as a superoxide quencher. Valuable experimental evidence, including RRDE measurements, LiO_2 retention detected by EPR, and morphological analysis of the discharge products from different discharge modes, were also provided to substantiate this reaction pathway. Consequently, as a bifunctional superoxide quencher, EV^+ promotes the surface reaction route in Li-O_2 batteries without compromise of capacity, which may contribute to a stable cycling with negligible side reactions. The preserved high capacity, which seemingly contradicts the

prevailed understanding of surface reaction route, can be an intriguing aspect to investigate in the future.

ACKNOWLEDGEMENTS

This work was supported by the National Natural Science Foundation of China (No. 21875097, No. 21671096), the Shenzhen Key Laboratory of Interfacial Science and Engineering of Materials (No. ZDSYS20200421111401738), the National Research Foundation, Singapore under Award No. NRF-CRP24-2020-0002 and No. NRF-NRFI2018-06, and Singapore A*STAR SERC CRF Award. The use of computing resources at the A*STAR Computational Centre and National Supercomputer Centre, Singapore is gratefully acknowledged. The Southern University of Science and Technology Core Research Facilities is also acknowledged for the physical characterizations.

REFERENCES

1. Yang, Z.; Zhang, J.; Kintner-Meyer, M. C.; Lu, X.; Choi, D.; Lemmon, J. P.; Liu, J., Electrochemical Energy Storage for Green Grid. *Chem. Rev.* **2011,** *111*, 3577-3613.
2. Kwak, W. J.; Rosy; Sharon, D.; Xia, C.; Kim, H.; Johnson, L. R.; Bruce, P. G.; Nazar, L. F.; Sun, Y. K.; Frimer, A. A.; Noked, M.; Freunberger, S. A.; Aurbach, D., Lithium-Oxygen Batteries and Related Systems: Potential, Status, and Future. *Chem Rev* **2020,** *120* (14), 6626-6683.
3. Li, Y.; Lu, J., Metal–Air Batteries: Will They Be the Future Electrochemical Energy Storage Device of Choice? *ACS Energy Letters* **2017,** *2*, 1370-1377.
4. Imanishi, N.; Luntz, A. C.; Bruce, P., *The Lithium Air Battery- Fundamentals*. Springer: New York, 2014.
5. Liu, T.; Vivek, J. P.; Zhao, E. W.; Lei, J.; Garcia-Araez, N.; Grey, C. P., Current Challenges and Routes Forward for Nonaqueous Lithium-Air Batteries. *Chem. Rev.* **2020,** *120* (14), 6558-6625.
6. Tan, P.; Jiang, H. R.; Zhu, X. B.; An, L.; Jung, C. Y.; Wu, M. C.; Shi, L.; Shyy, W.; Zhao, T. S., Advances and challenges in lithium-air batteries. *Applied Energy* **2017,** *204*, 27.
7. Geng, D.; Ding, N.; Hor, T. S. A.; Chien, S. W.; Liu, Z.; Wuu, D.; Sun, X.; Zong, Y., From Lithium-Oxygen to Lithium-Air Batteries: Challenges and Opportunities. *Advanced Energy Materials* **2016,** *6*, 1502164.
8. Li, F.; Zhang, T.; Zhou, H., Challenges of Non-Aqueous Li–O_2 Batteries: Electrolytes, Catalysts, and Anodes. *Energy & Environmental Science* **2013,** *6* (4), 1125.
9. Feng, N.; He, P.; Zhou, H., Critical Challenges in Rechargeable Aprotic Li-O_2 Batteries. *Advanced Energy Materials* **2016,** *6*, 1502303.

10. Chen, Y.; Freunberger, S. A.; Peng, Z.; Fontaine, O.; Bruce, P. G., Charging a Li-O_2 Battery Using a Redox Mediator. *Nat. Chem.* **2013,** *5*, 489-494.
11. Bergner, B. J.; Schurmann, A.; Peppler, K.; Garsuch, A.; Janek, J., TEMPO: a Mobile Catalyst for Rechargeable Li-O_2 Batteries. *J. Am. Chem. Soc.* **2014,** *136* (42), 15054-15064.
12. Zhu, Y. G.; Jia, C.; Yang, J.; Pan, F.; Huang, Q.; Wang, Q., Dual Redox Catalysts for Oxygen Reduction and Evolution Reactions: Towards a Redox Flow Li-O_2 Battery. *Chem. Commun.* **2015,** *51*, 9451-9454.
13. Zhu, Y. G.; Wang, X.; Jia, C.; Yang, J.; Wang, Q., Redox-Mediated ORR and OER Reactions: Redox Flow Lithium Oxygen Batteries Enabled with a Pair of Soluble Redox Catalysts. *ACS Catalysis* **2016,** *6* (9), 6191-6197.
14. Yang, L.; Frith, J. T.; Garcia-Araez, N.; Owen, J. R., A New Method to Prevent Degradation of Lithium-Oxygen Batteries: Reduction of Superoxide by Viologen. *Chem. Commun.* **2015,** *51* (9), 1705-1708.
15. Lim, H. D.; Song, H.; Kim, J.; Gwon, H.; Bae, Y.; Park, K. Y.; Hong, J.; Kim, H.; Kim, T.; Kim, Y. H.; Lepro, X.; Ovalle-Robles, R.; Baughman, R. H.; Kang, K., Superior Rechargeability and Efficiency of Lithium-Oxygen Batteries: Hierarchical Air Electrode Architecture Combined with a Soluble Catalyst. *Angew Chem Int Ed Engl* **2014,** *53* (15), 3926-3931.
16. Zhang, P.; Liu, L.; He, X.; Liu, X.; Wang, H.; He, J.; Zhao, Y., Promoting Surface-Mediated Oxygen Reduction Reaction of Solid Catalysts in Metal-O_2 Batteries by Capturing Superoxide Species. *J. Am. Chem. Soc.* **2019,** *141* (15), 6263-6270.
17. Gao, X.; Chen, Y.; Johnson, L.; Bruce, P. G., Promoting Solution Phase Discharge in Li-O_2 Batteries Containing Weakly Solvating Electrolyte Solutions. *Nat Mater* **2016,** *15* (8), 882-888.
18. Sun, D.; Shen, Y.; Zhang, W.; Yu, L.; Yi, Z.; Yin, W.; Wang, D.; Huang, Y.; Wang, J.; Wang, D.; Goodenough, J. B., A Solution-Phase Bifunctional Catalyst for Lithium-Oxygen Batteries. *J. Am. Chem. Soc.* **2014,** *136* (25), 8941-8946.
19. Wu, S.; Qin, N.; Zhang, H.; Wei, C.; Wang, Z.; Luo, W.; Li, Y.; Wang, H.; Zhang, K.; Wang, Q.; Lu, Z., Revealing the catalytic pathway of a quinone-mediated oxygen reduction reaction in aprotic Li–O2 batteries. *Chemical Communications* **2022,** *58* (7), 1025-1028.
20. Ryu, W.-H.; Gittleson, F. S.; Thomsen, J. M.; Li, J.; Schwab, M. J.; Brudvig, G. W.; Taylor, A. D., Heme Biomolecule as Redox Mediator and Oxygen Shuttle for Efficient Charging of Lithium-Oxygen Batteries. *Nature Communications* **2016,** *7*, 12925.
21. Zhang, Y.; Wang, L.; Zhang, X.; Guo, L.; Wang, Y.; Peng, Z., High-Capacity and High-Rate Discharging of a Coenzyme Q10-Catalyzed Li-O_2 Battery. *Adv. Mater.* **2018,** *30*, 1705571.
22. Zhu, Y. G.; Goh, F. W. T.; Yan, R.; Wu, S.; Adams, S.; Wang, Q., Synergistic Oxygen Reduction of Dual Redox Catalysts Boosting the Power of Lithium-Air Battery. *Phys. Chem. Chem. Phys.* **2018,** *20*, 27930-27936.
23. Wan, H.; Sun, Y.; Li, Z.; Wang, W.; Zhu, Y.; Qian, Y., Satisfying Both Sides: Novel Low-Cost Soluble Redox Mediator Ethoxyquin for High Capacity and Low Overpotential Li-O_2 Batteries. *Energy Storage Materials* **2021,** *40*, 159-165.
24. Xiong, Q.; Huang, G.; Zhang, X. B., High-Capacity and Stable Li-O2 Batteries Enabled by a Trifunctional Soluble Redox Mediator. *Angew Chem Int Ed Engl* **2020,** *59* (43), 19311-19319.
25. Lau, K. C.; Lu, J.; Luo, X.; Curtiss, A. L.; Amine, K., Implications of the Unpaired Spins in Li–O_2 Battery Chemistry and Electrochemistry: A Minireview. *ChemPlusChem* **2015,** *80*, 336-343.

26. Lu, J.; Jung, H. J.; Lau, K. C.; Zhang, Z.; Schlueter, J. A.; Du, P.; Assary, R. S.; Greeley, J.; Ferguson, G. A.; Wang, H. H.; Hassoun, J.; Iddir, H.; Zhou, J.; Zuin, L.; Hu, Y.; Sun, Y. K.; Scrosati, B.; Curtiss, L. A.; Amine, K., Magnetism in Lithium-Oxygen Discharge Product. *ChemSusChem* **2013,** *6*, 1196-1202.
27. Gittleson, F. S.; Jones, R. E.; Ward, D. K.; Foster, M. E., Oxygen solubility and transport in Li–air battery electrolytes: establishing criteria and strategies for electrolyte design. *Energy & Environmental Science* **2017,** *10* (5), 1167-1179.
28. Das, U.; Lau, K. C.; Redfern, P. C.; Curtiss, L. A., Structure and Stability of Lithium Superoxide Clusters and Relevance to Li-O_2 Batteries. *J. Phys. Chem. Lett.* **2014,** *5* (5), 813-819.
29. Xiong, Q.; Huang, G.; Zhang, X. B., High-Capacity and Stable Li-O_2 Batteries Enabled by a Trifunctional Soluble Redox Mediator. *Angew. Chem. Int. Ed. Engl.* **2020,** *59* (43), 19311-19319.